



Development of microtextures on polymer surfaces using the transfer method from metal templates

Oleksiy Myronyuk

Doctor of Technical Sciences, Associate Professor

National Technical University of Ukraine "Igor Sikorsky Kyiv Polytechnic Institute"

03056, 37 Beresteyskyi Ave., Kyiv, Ukraine

<https://orcid.org/0000-0003-0499-9491>

Denys Baklan

PhD

National Technical University of Ukraine "Igor Sikorsky Kyiv Polytechnic Institute"

03056, 37 Beresteyskyi Ave., Kyiv, Ukraine

<https://orcid.org/0000-0002-6608-0117>

Anna Bilousova*

Postgraduate Student

National Technical University of Ukraine "Igor Sikorsky Kyiv Polytechnic Institute"

03056, 37 Beresteyskyi Ave., Kyiv, Ukraine

<https://orcid.org/0000-0002-2818-8450>

Volodymyr Strashenko

Postgraduate Student

National Technical University of Ukraine "Igor Sikorsky Kyiv Polytechnic Institute"

03056, 37 Beresteyskyi Ave., Kyiv, Ukraine

<https://orcid.org/0009-0009-3601-1821>

Abstract. Scaling up technologies for creating relief surfaces with controlled wetting properties is a pressing issue for the development of functional polymer materials. There is a need to investigate the patterns of transfer of micro- and nanotextures from metal templates to polymer substrates. The purpose of the study was to determine the influence of the replication method and polymer properties on the accuracy of relief reproduction and the development of water-repellent surface characteristics. Three replication methods were used for this purpose: obtaining polycarbonate film from a solution, reaction moulding using polydimethylsiloxane elastomer, and thermoforming of polyethylene films. The negative copies obtained were used as intermediate forms (polycarbonate) for creating positive replicas from polyethylene and polysiloxane. The hydrophobicity of the materials was evaluated by measuring the contact angles in directions parallel and perpendicular to the texture orientation. The results showed that all methods ensure the reproduction of periodic structures. However, the level of accuracy depends on the viscosity of the medium and the temperature conditions, with the lowest level of accuracy observed for polycarbonate and the highest level observed for polyethylene. Polycarbonate negatives were characterised by high detail of microdefects (up to 5 μm), while polyethylene films showed smoothing of the relief. Silicone positives most fully preserved the geometry of the original textures with defects. The study of surface hydrophobicity showed a significant increase in contact angles on structured surfaces compared to smooth ones, especially with parallel orientation. The maximum contact angles reached 140°C for polysiloxane and 139°C for polyethylene replicas of the structure with regular grooves. The practical significance of the study lay in identifying the optimal materials and methods for creating polymer surfaces with increased water repellency. Polycarbonate is suitable for use as an intermediate material for accurate texture copying, while silicone and polyethylene have potential for use as functional surfaces in protective coatings and liquid-infused porous surfaces

Keywords: contact angle; polycarbonate; silicone; polyethylene; hydrophobicity

Suggested Citation:

Myronyuk, O., Baklan, D., Bilousova, A., & Strashenko, V. (2025). Development of microtextures on polymer surfaces using the transfer method from metal templates. *Technologies and Engineering*, 26(4), 44-53. doi: 10.30857/2786-5371.2025.4.4.

* Corresponding author



Introduction

Liquid-infused porous surfaces (LIPS) combine a porous or textured substrate with a lubricating liquid, enabling stable repellent behaviour in conditions where conventional superhydrophobic coatings prove unreliable. Such surfaces have found application in areas such as corrosion protection and anti-icing. It is the combination of stability under dynamic impact, resistance to condensation, and layer renewability that makes these surfaces a promising technology for large-scale solutions. Y. Meng *et al.* (2025) reviewed that LIPS materials represent an advancement of previously known textured surfaces which, upon reaching a Cassie state, could exhibit superhydrophobicity – characterised by water contact angles exceeding 150°. I.W. Park *et al.* (2023) reviewed that LIPS properties such as self-cleaning, water repellency, and resistance to ice formation are ensured by the Cassie-Baxter wetting state, which is achieved by high surface roughness and low surface energy of the material itself.

G. McHale *et al.* (2023) characterised significant drawbacks that served as fundamental limitations to practical application of LIPS. A limited range of liquid surface tensions was exhibited with which they could effectively repel. When the surface tension of a liquid dropped below this threshold, a transition occurred from the Cassie-Baxter state to the Wenzel state. H. Xie & H. Huang (2020) described this transition as a result in partial surface wetting, with liquid penetrating and being retained within the texture grooves – an effect directly opposite to the intended purpose of such surfaces for liquid repellency. In addition, D. Tripathi *et al.* (2023) found that LIPS are dynamically unstable. Specifically, when a droplet of wetting liquid hit them at a certain speed, it could change the state from Cassie-Baxter to Wenzel. Additionally, such surfaces were unstable against water vapour condensation. S. Adera *et al.* (2021) showed that in humid atmospheres, the enhanced water-repellent properties associated with superhydrophobicity diminished over time.

S. Peppou-Chapman *et al.* (2020) reviewed drawbacks of LIPS. Their water-repellent performance is lower than that of superhydrophobic surfaces because the infusion liquid's polarity is higher than air's. They are more stable than other surfaces, however, this is conditioned by their lack of open cavities that could be filled by water. Q. Cai *et al.* (2023) described that LIPS fabrication technologies are similar to those for superhydrophobic surfaces. They rely on the same methods to produce the structural layer that retains the infusion liquid. Sponges, electrospun surfaces, nonwoven materials, and porous substrates can be used as porous media. I.N. Etim *et al.* (2025) researched LIPS fabrication methods. These methods have the same drawback as for superhydrophobic surfaces: their widespread adoption and practical implementation are significantly limited by the inherently low scalability of the available fabrication techniques. P. Gao *et al.* (2023) showed that texture transfer by injection moulding of polypropylene and polymethyl methacrylate is a promising method for obtaining textured materials that are wettable according

to the Cassie-Baxter state. The proposed method is inexpensive and easily scalable, although obtaining a shape with the required hierarchical structure has low productivity and high cost due to laser processing.

Challenges may arise during the texture transfer from metallic substrates to polyethylene and subsequently to polydimethylsiloxane, particularly regarding the loss of original structural features. This investigation focused on transfer fidelity and geometric discrepancies between successive replicas. Thus, the primary objective of this study was to investigate the regularities governing texture transfer from metallic templates onto polyethylene and polydimethylsiloxane (PDMS) substrates, using thermocompression, solution castings, and reactive moulding techniques, respectively.

Materials and Methods

The present study addressed the fabrication of scalable liquid-retaining structural layers using thermoforming and reactive curing techniques. Polyethylene was selected for thermocompression due to its low polarity, cost, and availability, while PDMS served as a reactive material capable of accurately reproducing surface textures. Stainless steel (AISI 304) plates textured by femtosecond laser were used as primary moulds, creating microstructures with features up to 10 µm and groove depths of 20-30 µm. Such laser texturing can also generate secondary periodic features that influence polymer melt and interfacial adhesion, an effect further examined in this study.

Although laser texturing created well-defined protrusions, the bottom of the grooves often formed unpredictable conical depressions that appeared as unwanted protrusions on the reproduced polymer surfaces (Bonse *et al.*, 2021). To minimise these artefacts, an intermediate replica layer was introduced between the metal template and polyethylene. Polycarbonate was chosen for this purpose due to its high melting point, good mouldability, and ease of dissolution in common solvents. Its low adhesion to metal surfaces (Du *et al.*, 2023) also facilitated defect-free separation of moulded films.

The basic textures on the surface of steel were obtained by femtosecond laser ablations described in previous paper (Myronyuk *et al.*, 2023) with parameters shown in Table 1. This study was designed to investigate the relationship between the quality of microtexture transfer from metal templates to polymer materials. The quality of microtexture geometry replication on the surface, compared replication techniques, and compared the wettability of the resulting textured surfaces were evaluated. The study employed a combination of experimental and analytical methods, including replication via solution casting, reactive moulding, and thermal embossing. This was followed by microscopic characterisation and contact angle analysis. The overall methodology was based on a comparative evaluation of textured samples obtained using different replication methods while maintaining substrate topographies.

Table 1. Parameters of the texture grooves

Texture	Material	Type	Groove width, μm	Groove depth, μm	Texture period, μm
A	AISI304	positive	24.8 ± 2	19.5 ± 1	60 ± 2
B	AISI304	positive	40 ± 1	24.5 ± 2	60 ± 1

Source: O. Myronyuk *et al.* (2023)

In this study, three methods were employed to replicate textures from metallic templates:

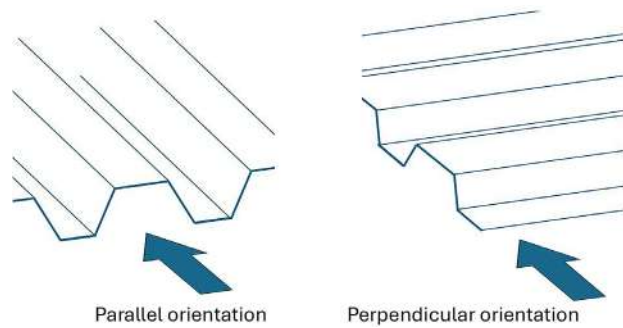
1) A solution-based approach involved the use of a 5 wt. % dichloromethane solution of polycarbonate Calibre 303 10 TNT (Dow Chemicals). This solution was cast onto the surface of the textured metallic plate and left at room temperature for 1 h. to allow dichloromethane evaporation. To ensure complete removal of residual solvent, the samples were subsequently placed in a drying oven at 80°C for an additional 3 h. The resulting films were detached from the metallic templates due to shrinkage during solvent evaporation.

2) Reactive moulding method was performed using a polydimethylsiloxane elastomer. A two-component, platinum-catalysed, addition-curing PDMS system (SKA 035man. Silikony SK, Slovak Republic) was employed. After mixing, the liquid reactive composition was poured onto the surface of the textured sample, with the edges confined by a polyethylene ring. The assembly was then subjected to vacuum treatment to remove entrapped air. Following this step, the specimen was left to cure for 3 days, after which the silicone negative was carefully detached from the metallic plate.

3) A thermal moulding method (thermo-pressing) was performed by heating of metallic templates using a magnetic stirrer heater (RIVA-03.6, UOSLAB, Ukraine) to approximately 115°C. A low-density polyethylene film was then placed onto the heated surface and rolled with a polyurethane roller to ensure complete imprinting of the structure. Following this step, the template was carefully removed from the plate, allowed to cool to room temperature, and the textured polyethylene layer was mechanically detached.

The textures obtained by these methods were referred to as negative, as they represented inverse replicas of the original positive textures present on the metallic templates. To obtain positive replicas – specifically from polydimethylsiloxane, polyethylene, and polycarbonate – the polycarbonate negative was employed as the intermediate template. In this approach, thermoforming with polyethylene was carried out not on the metallic plate but on the polycarbonate negative, taking advantage of the fact that the melting temperature of polycarbonate is significantly higher than that of polyethylene. A similar procedure was applied during reactive curing: the PDMS mixture was cast onto the surface of the polycarbonate negative and left to cure under the same conditions as those used with the metallic template. To obtain a polycarbonate positive, the same polycarbonate solution described earlier was employed. However, instead of casting onto the metallic template, the solution was applied onto a PDMS negative, which served as the replication substrate.

The water contact angle was measured using the combination of Konus Academy 2 (Italy) optical microscope with goniometric setup and digital camera UCMOS 1300 (Sigeta) images were processed using the ToupView software (ToupTek). The same complex was used for obtaining the optical microscopy images of the microtextured surfaces. In this study, extended textures oriented along a single axis were employed. Of particular interest was the evaluation of wetting behaviour in two orthogonal directions, namely parallel and perpendicular to the texture orientation. Accordingly, throughout this study these areas were referred to as the parallel and perpendicular orientations, as schematically illustrated in Figure 1. Deionised water and dichloromethane (solvent for polycarbonate) were used as supplementary materials in this study.

**Figure 1.** Water contact angle measurement directions

Source: developed by the authors of this study

Overall, the experimental procedure involved several sequential stages: (1) generation of primary laser-induced textures on steel templates; (2) replication of these textures into polymeric negative; (3) fabrication of positive polysiloxane and polyethylene replicas through moulding; and (4) characterisation of surface morphology and wetting behaviour in orthogonal directions. This structure ensured a consistent framework for comparing replication accuracy and material-specific behaviour under identical texturing conditions. Such an approach allowed for a comprehensive methodological assessment of the efficiency and reproducibility of polymer texture transfer processes.

Results and Discussion

The textures that were used as metal templates (Fig. 2) have a linear grooves pattern divided with asperities. For the texture A, the period is well-reproduced 60 μm with the groove width 25 μm . The asperity has a larger width – 35 μm . In the case of this structure, the grooves have the profile of a reverse triangle with the height of 19 μm . Even in optical microscopy photos it is seen that the sides of these

triangles are irregular due to the uneven removal of the material during the laser ablation. The texture B has the same period – 60 µm, but a significantly wider groove that is 45 µm with the asperity width 15 µm. It is seen that the groove in this case has the inverse trapezoid profile with small diameter holes on the bottom. These holes may be seen in both A and B textures and are typically formed at the places of the laser beam focusing. Thus, as evident from the texture images, the groove surfaces appear highly heterogeneous. They exhibit distinct artefacts and localised accumulations of material. Moreover, closer inspection reveals that the ridges themselves are far from perfectly smooth. Together, these two factors pose significant challenges when attempting to replicate such surfaces with high fidelity.

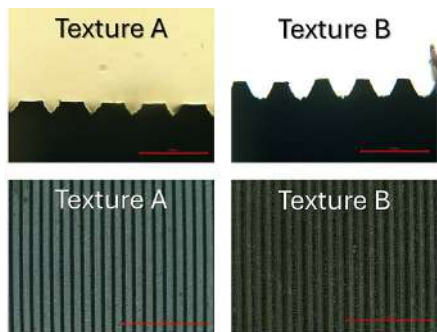


Figure 2. Optical microscopy images

Source: developed by the authors of this study based on the findings of experimental research

As illustrated in Figure 3, laser-induced textures were successfully transferred onto polymer substrates by three methods: reactive curing for silicone, solution casting for polycarbonate, and thermo-pressing for polyethylene. Each approach resulted in a clearly defined surface structure, enabling further comparison of replication fidelity and wetting behaviour. It can be concluded that all the replication methods enable a sufficiently accurate transfer of the texture. In particular, the periodicity was preserved, along with the regularity of the pattern and the groove width at the upper surface of the texture. When examining not only the top view of the textures but also their cross-sectional profiles, it became evident that different replication methods yield varying levels of fidelity. For instance, on polycarbonate negative, the apexes of the pyramidal structures were encrusted with artefactual formations originating from the focal points of the laser. These artefacts are relatively large – reaching up to 5 µm in height – and are distributed in a disordered manner across the surface. Similar artefactual formations can be observed for other samples. For polyethylene negative the pyramidal structures appear significantly narrower. This effect is primarily attributed to the use of an alternative template design featuring much narrower grooves. Notably, the artefactual formations have nearly disappeared, indicating that across the sequence of polycarbonate-polysiloxane-polyethylene there is a progressive reduction in the size of these extraneous features.

This trend can likely be explained by the progressive increase in viscosity of the medium used for texture replication, moving from polycarbonate solution to liquid silicone resin and ultimately to molten polyethylene.

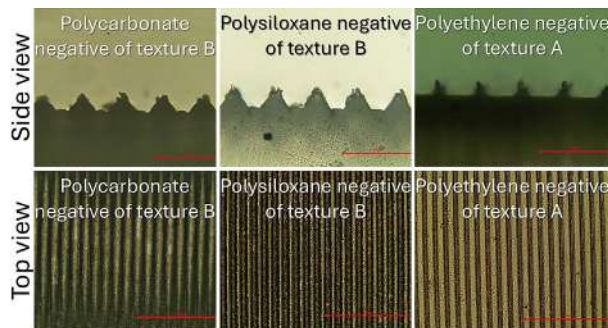


Figure 3. Textures obtained by templating from metal matrices

Source: developed by the authors of this study based on the findings of experimental research

Consequently, the lowest-viscosity system – namely, the polycarbonate solution in dichloromethane – exhibited the greatest ability to reproduce the fine surface features of the template with high fidelity. It should be emphasised that the presence of such artefactual formations on the textured surface is an undesirable factor. As demonstrated in earlier study by O. Myronyuk *et al.* (2024), these protrusions effectively reduce the maximum attainable water contact angle by destabilising the Cassie-Baxter state. They are expected to influence another critical parameter – the sliding angle strongly. Following the mechanism observed in the “rose petal” effect, these features enhance droplet pinning of the wetting liquid, thereby increasing the sliding angle. Thus, their presence is detrimental to the overall wetting performance of the surface. As can be seen from Figure 3, these artefacts are characteristic of nearly all surface replication methods employed. Consequently, relying solely on negative moulding from the template does not allow for the production of high-quality replicas with complete structural fidelity. Therefore, the authors of this study adopted a somewhat different approach. First, a negative template was prepared by a solution-based method using polycarbonate. This negative was then employed to generate positive structures from both a silicone polymer and polyethylene. In the former case, the replication was achieved through reactive moulding, while in the latter it was accomplished by thermo-pressing.

As shown in Figure 4, the positive replicas reproduced the original structure of the source templates with considerable accuracy compared to the metal substrates. Deep and highly accurate reproduction was achieved in both cases using polysiloxane polymer. This effect is particularly noticeable for texture A, where the dimensional characteristics are virtually identical to those of the original metal template, despite the fact that the structure was transferred through an intermediate polycarbonate negative.

The positive replica of texture B on polysiloxane differs slightly from the original template due to the presence of artificial concavity on the surface of the textured elements. Notably, this concavity is also present to a lesser extent in the original metal templates. The polyethylene replicas appeared less accurate, partly due to the visualisation conditions. In terms of dimensionality and geometry, it should be noted that the structural period and the crest-to-groove ratio remained unchanged for polyethylene and polysiloxane. The depth of the grooves was almost the same as that of the original structure. However, the angles and features were noticeably less distinct compared to the silicone body. This result was expected, as molten polyethylene has a significantly higher viscosity than liquid silicone during the moulding of these replicas.

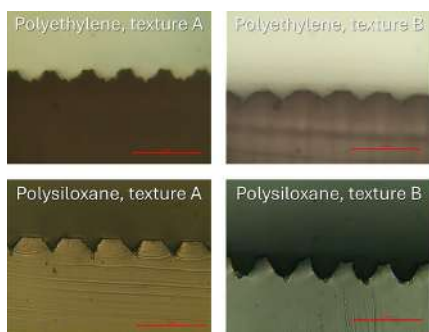


Figure 4. Side view of positive textures

Source: developed by the authors of this study based on the findings of experimental research

The parameters of structure transfer from the metallic master templates (AISI304) with texture A and texture B onto polymer surfaces were presented in Table 2. Based on the data in the table, it is important to note that the negatives were obtained through direct contact of the polymers with the metallic templates, whereas the positives were produced by casting polyethylene and PDMS onto the surface of the polycarbonate negative. As a result, they also

inherited the imprint of this intermediate template along with its associated modifications. For texture B, the polycarbonate negative exhibited certain alterations compared to the original template. First, there was a slight reduction in the height of the protrusions, although this decrease remained within the margin of experimental error. The textures exhibited a slight reduction in height, which can be attributed to the shrinkage of the polymer film following solvent evaporation. Moreover, it was observed that the width corresponding to the groove dimension in the positive replica remained unchanged, consistently measuring around 40 μm . The polysiloxane negative reproduced the template structure with nearly the same accuracy as the solution-cast polycarbonate. The only noticeable difference was that the grooves appear slightly deeper than those in the polycarbonate replica. However, this variation lied within the margin of error and can reasonably be attributed to statistical deviation.

The positive structures were of particular interest, as they represented the intended functional surfaces. Notably, the polysiloxane positive exhibited a slightly greater groove width, which arises from the corresponding broadening of the ridge elements in this replication process. Here, the difference was modest – 44 μm compared to 40 μm – yet it already lied beyond the range of statistical error. Thus, it can be concluded that during the moulding process certain effects, such as elongation upon demoulding or shrinkage, lead to a measurable narrowing of the ridge elements. This observation was further supported by the fact that the height of these ridges increased to 26.5 μm . However, the opposite trend was observed in another positive replica. Here, the ridge height decreased to approximately 20.5 μm , a change that also falls outside the bounds of statistical error. In addition, the ridge width showed a slight increase, although this variation remained within the margin of experimental uncertainty. Similar trends were also observed for texture A. Taller and more elongated ridges characterise the siloxane positive, whereas the polyethylene positive exhibits comparatively shorter ridge structures.

Table 2. Parameters of the texture grooves

Texture	Material	Type	Groove width, μm	Groove depth, μm	Texture period, μm
A	AISI304	positive	24.8 \pm 2	19.5 \pm 1	60 \pm 2
B	AISI304	positive	40 \pm 1	24.5 \pm 2	60 \pm 1
A	Polyethylene	positive	36.5 \pm 2	18.5 \pm 1	58 \pm 2
A	Polyethylene	negative	25.0 \pm 1	23 \pm 1.5	60 \pm 1
B	Polyethylene	positive	37.5 \pm 1.5	20.5 \pm 1	58 \pm 2.5
A	Polysiloxane	positive	30.0 \pm 2	22.0 \pm 1.5	59.5 \pm 2
B	Polysiloxane	positive	44.5 \pm 1.5	26.5 \pm 2	58 \pm 2.5
B	Polysiloxane	negative	39.0 \pm 1.5	25.5 \pm 2	57 \pm 2.5
B	Polycarbonate	negative	39.5 \pm 1.5	22.0 \pm 1	57 \pm 2.5

Note: negatives of polyethylene, silicone, and polycarbonate are presented only for texture "B" for the purpose of comparing transfer quality

Source: developed by the authors of this study based on the findings of experimental research

For the development of infused-liquid surfaces and superhydrophobic coatings, the key characteristics were

defined by the wetting behaviour of the surface. This study examined how water wettability varies depending on the type

of structures that were fabricated. As shown in Table 3, the presence of surface texturing generally leads to an increase in the water contact angle of the materials in most cases. The flat surfaces exhibited a maximum water contact angle of approximately 103°, observed for polydimethylsiloxane. The textured surfaces exhibited enhanced contact angles regardless of whether they represented positive or negative replicas. The general trend showed that the perpendicular

contact angles were only moderately higher than those of the flat surfaces, whereas in the case of parallel textures, the contact angles were significantly larger – by as much as 40° compared to the flat reference. This increase can primarily be attributed to the grooves themselves, which act as barriers to the spreading of the test liquid, in this case water, thereby generating a pronounced advancing angle that manifests as the measured static contact angle.

Table 3. Parameters of the texture grooves

Texture	Material	Type	Orientation	Water contact angle, °
-	Polycarbonate	-	-	86.8 ± 2.2
-	Polyethylene	-	-	92.8 ± 0.6
-	Polysiloxane	-	-	102.7 ± 3.9
A	Polyethylene	positive	perpendicular =	102.4 ± 6.9
			parallel	130.6 ± 2.2
			perpendicular =	137.4 ± 1.3
			parallel	138.8 ± 2.5
B	Polysiloxane	positive	perpendicular =	114.5 ± 1.7
			parallel	133.8 ± 2.1
			perpendicular =	125.6 ± 0.9
			parallel	139.1 ± 1
A	Polycarbonate	negative	perpendicular =	91.0 ± 4.6
			parallel	127.4 ± 0.65
			perpendicular =	60.7 ± 5.4
			parallel	111.2 ± 5.4

Note: “-” denotes samples without texture

Source: developed by the authors of this study based on the findings of experimental research

When comparing the efficiency of structures A and B, specifically their positive replicas, structure B proved to be more effective. In the parallel orientation, the polysiloxane sample – the most non-polar material – exhibited a maximum contact angle of approximately 140°, while polyethylene reached 139°. By contrast, structure A showed a lower maximum value, with the contact angle limited to about 134°. Based on data presented in Table 3, it can be concluded that the most effective configuration for enhancing water repellency is the positive replica based on structure B. Both polyethylene and polysiloxane proved to be highly promising materials for achieving elevated contact angles. In contrast, polycarbonate, owing to its higher polarity, is less effective in this regard. However, it serves excellently as an intermediate negative, as it reliably preserves the structural features of the original templates and enables the fabrication of highly reproducible positives from other polymers.

The results showed that the basic geometry of the textures was well preserved in all polymer replicas. However, artefacts with a diameter of up to 5 µm were observed at the top of the pyramidal elements in negative polycarbonate matrices, presumably due to the laser's action during focusing. Similarly, irregularities in replication were recorded in the study by V. Basile *et al.* (2022). Positive copies on polysiloxane were nearly identical to the original metal template; however, polyethylene replicas were less clear. The contours of the ridges were smoother, and the corners were less sharp due to the higher viscosity of

molten polyethylene during thermoforming (Lysenkov & Strutskiy, 2022). Generally, as viscosity increases, the size and number of artefacts decrease; however, the replication accuracy of small details deteriorates. This was consistent with the observation of C. Sáez-Comet *et al.* (2022) that decreasing polymer viscosity (e.g., by increasing temperature) improves penetration into fine grooves and increases microtexture copying accuracy. Some parameters of the replicas differed systematically from the original. For instance, the width of the ridges in the polysiloxane positive for texture B increased from ~40 µm in the metal sample to ~44 µm, which can be explained by deformation during removal from the mould. The presence of artificial structures on surfaces can locally alter wetting angles, though it does not affect overall regularity. These differences suggest the effects of elastic recovery and shape change during cooling and material removal.

Surface texturing significantly increases the contact angle compared to flat samples. The Cassie-Baxter model explained this phenomenon: micro-roughness allows air to be retained in the depressions under the drop, increasing the macroscopic wetting angle (Ma *et al.*, 2024). Additionally, pronounced anisotropy of wetting was observed: the angles measured parallel to the grooves were significantly higher than those measured perpendicular to them. Similar anisotropic wetting results were observed with micro-rough PDMS surfaces in Q. Legrand *et al.* (2022). As expected, structure B provided a higher contact angle than

structure A because more open-air area leads to a higher effective wetting angle according to the Cassie-Baxter model. Additionally, the nonpolar polysiloxane and polyethylene used to create the positives exhibited higher angles than the polar polycarbonate, consistent with these principles.

The presence of microartefacts was undesirable for water-repellent properties. As shown in the study by J. Bai *et al.* (2024), this leads to the “petal effect” a high static angle with high hysteresis. In other words, the surface becomes “stickier” for droplets. Contrary to the “lotus effect” irregularities impede the movement of the droplet. Y.B. Chatenet & S. Valette (2024) simulated the “lotus effect” and “petal effect” and showed that fluid penetration between irregularities in such micro-roughness leads to a decrease in the contact angle. Authors observations coincide with this: the presence of artefacts reduces the effectiveness of achieving the Cassie-Baxter state and increases excess hydrodynamic resistance. Therefore, smoothing or eliminating these structures is critical to manufacturing highly efficient superhydrophobic surfaces.

Thus, for the further advancement of research in this field, several strategies are recommended to enhance the water-repellent performance of textured surfaces. P. Gao *et al.* (2023) showed that the replication rate correlates with the viscosity of the polymer melt, which ensures a higher degree of polypropylene replication. D. Masato *et al.* (2022) proved that polymer deformation must be considered when separating the polymer from the metal template. Additionally, J. Krantz *et al.* (2022) proved in their study that the influence of temperature is significant. Thus, the use of lower-viscosity materials during moulding should be prioritised, which in thermoforming can be achieved either by increasing the processing temperature or by applying higher moulding pressure. The resulting textured surfaces may be further improved through post-processing hydrophobisation. I. Ramos *et al.* (2025) showed that the use of PDMS to impart hydrophobicity provides efficiency and durability. N. Rungruangkitkrai *et al.* (2024) showed that PDMS is a good alternative to fluorinated modifiers for creating LIPS materials. Although both polyethylene and PDMS are relatively nonpolar materials, they still possess a degree of surface polarity, and their hydrophobic properties can be significantly enhanced by additional surface modification.

Structure B provides higher contact angles than structure A, especially with less polar polymers like polysiloxane and polyethylene. Microtexture geometry is generally preserved during replication, though local microartefacts and deformations due to polymer viscosity and elastic recovery reduce accuracy. This aligns with the Cassie-Baxter model, which explains the increase in the contact angle due to air retention in microcavities and confirms the role of surface structure and material polarity in controlling wetting. Micro-irregularities beyond regular texture lead to a “petal” effect with increased hysteretic adhesion, reducing water-repellent properties. Optimising polymer melt viscosity during forming, controlling deformations during demoulding, and additional surface

hydrophobisation are key strategies for improving superhydrophobic textured coatings.

Conclusions

The possibility of texture transfer onto polymer surfaces from textured metallic templates was demonstrated. The fidelity of replication is strongly influenced by the viscosity of the medium. Better replication quality was for polycarbonate solution. The accuracy of structure transfer increases to 5 µm with a decrease in viscosity, such as when switching from polymer melts and reactive mixtures to polymer solutions. In this study, a successful technological combination was demonstrated, whereby negatives were first fabricated by solution casting of polycarbonate, and these negatives were subsequently employed as templates for producing positive textured surfaces from polyethylene and polydimethylsiloxane.

During such transfers, the replicated structures exhibited distinct trends when compared to the original metallic substrates. First, the spacing between the texture ridges increased significantly – by up to 50% – and this effect was more pronounced for texture A (groove width 25 µm, groove depth 20 µm) than for texture B (groove width 40 µm, groove depth 25 µm). The increase was also more evident in the case of the highly viscous polyethylene than for polydimethylsiloxane, with changes of 50% and 25%, respectively. For texture B, the enlargement was much smaller, limited to about 10%. By contrast, the ridge height showed far less variation, with noticeable changes observed primarily in the polyethylene replicas.

It has been shown that surface texturing of polyethylene and PDMS leads to a substantial enhancement of their water-repellent properties. For instance, compared to flat polydimethylsiloxane, which exhibits a contact angle of 102°, the textured surfaces achieved values approaching 140°. This corresponded to an increase of close to 40° in the contact angle, clearly demonstrating the pronounced effect of texturing on wettability. The anisotropy of the texture also gives rise to anisotropy in the measured contact angles. For example, in the parallel orientation the contact angle reached approximately 140° for both polyethylene and polydimethylsiloxane, whereas in the perpendicular orientation the values decreased to approximately 125° and 137°, respectively. Further research should focus on determining the stability of infusion fluids in different textures and assessing their long-term stability under cyclic mechanical and chemical influences. These efforts will contribute to the practical applicability of slippery liquid-infused porous surface technology in operational conditions.

Acknowledgements

None.

Funding

This study was funded within the scope of the project # 2025.06/0031 “Polymeric liquid-infused films with de-icing

capability" (contract No. 217.0031 01.08.2025) by the National Research Foundation of Ukraine.

None.

Conflict of Interest

References

- [1] Adera, S., Naworski, L., Davitt, A., Mandsberg, N.K., Shneidman, A.V., Alvarenga, J., & Aizenberg, J. (2021). Enhanced condensation heat transfer using porous silica inverse opal coatings on copper tubes. *Scientific Reports*, 11, article number 10675. [doi: 10.1038/s41598-021-90015-x](https://doi.org/10.1038/s41598-021-90015-x).
- [2] Bai, J., Wang, X., Zhang, M., Yang, Z., & Zhang, J. (2024). Turning non-sticking surface into sticky surface: Correlation between surface topography and contact angle hysteresis. *Materials*, 17(9), article number 2006. [doi: 10.3390/ma17092006](https://doi.org/10.3390/ma17092006).
- [3] Basile, V., Modica, F., Surace, R., & Fassi, I. (2022). Micro-texturing of molds via Stereolithography for the fabrication of medical components. *Procedia CIRP*, 110, 93-98. [doi: 10.1016/j.procir.2022.06.019](https://doi.org/10.1016/j.procir.2022.06.019).
- [4] Bonse, J., Kirner, S.V., & Krüger, J. (2021). Laser-induced periodic surface structures (LIPSS). In K. Sugioka (Ed.), *Handbook of laser micro- and nano-engineering* (pp. 879-936). Cham: Springer. [doi: 10.1007/978-3-030-63647-0_17](https://doi.org/10.1007/978-3-030-63647-0_17).
- [5] Cai, Q., Xu, J., Yu, Z., Dong, L., Li, J., Lian, Z., & Yu, H. (2023). Fabrication of slippery liquid-infused porous surfaces on magnesium alloys with durable anti-corrosion and anti-tribocorrosion properties. *Colloids and Surfaces A: Physicochemical and Engineering Aspects*, 670, article number 131549. [doi: 10.1016/j.colsurfa.2023.131549](https://doi.org/10.1016/j.colsurfa.2023.131549).
- [6] Chatenet, Y.B., & Valette, S. (2024). Elucidating the lotus and rose-petal effects on hierarchical surfaces: Study of the effect of topographical scales on the contact angle hysteresis. *Journal of Colloid and Interface Science*, 676, 355-367. [doi: 10.1016/j.jcis.2024.07.114](https://doi.org/10.1016/j.jcis.2024.07.114).
- [7] Du, B., Zhou, X., Li, Q., Liu, J., Liu, Y., Zeng, X., Cheng, X., & Hu, H. (2023). Surface treat method to improve the adhesion between stainless steel and resin: A review. *ACS Omega*, 8(43), 39984-40004. [doi: 10.1021/acsomega.3c05728](https://doi.org/10.1021/acsomega.3c05728).
- [8] Etim, I.N., Zhang, R., Wang, C., Khan, S., Mathivanan, K., & Duan, J. (2025). New insights on slippery lubricant-infused porous surfaces technique in mitigating microbial corrosion. *Npj Materials Degradation*, 9, article number 34. [doi: 10.1038/s41529-025-00581-y](https://doi.org/10.1038/s41529-025-00581-y).
- [9] Gao, P., MacKay, I., Gruber, A., Krantz, J., Piccolo, L., Lucchetta, G., Pelaccia, R., Orazi, L., & Masato, D. (2023). Wetting characteristics of laser-ablated hierarchical textures replicated by micro injection molding. *Micromachines*, 14(4), article number 863. [doi: 10.3390/mi14040863](https://doi.org/10.3390/mi14040863).
- [10] Krantz, J., Caiado, A., Piccolo, L., Gao, P., Sorgato, M., Lucchetta, G., & Masato, D. (2022). Dynamic wetting characteristics of submicron-structured injection molded parts. *Polymer Engineering and Science*, 62(7), 2093-2101. [doi: 10.1002/pen.25983](https://doi.org/10.1002/pen.25983).
- [11] Legrand, Q., Benayoun, S., & Valette, S. (2022). Quantification and modeling of anisotropic wetting of textured surfaces. *Applied Surface Science*, 611(B), article number 155606. [doi: 10.1016/j.apsusc.2022.155606](https://doi.org/10.1016/j.apsusc.2022.155606).
- [12] Lysenkov, E., & Strutkyi, O. (2022). Electrical properties of polymer nanocomposites based on polyethylene oxide and silver nanoparticles in the area of low filler concentrations. *Bulletin of Cherkasy State Technological University*, 27(3), 94-101. [doi: 10.24025/2306-4412.3.2022.262507](https://doi.org/10.24025/2306-4412.3.2022.262507).
- [13] Ma, D., Liu, Z., Li, Y., & Luo, L. (2024). Experiment of droplet anisotropic wetting behavior on micro-grooved PDMS membranes. *Scientific Reports*, 14, article number 28011. [doi: 10.1038/s41598-024-78681-z](https://doi.org/10.1038/s41598-024-78681-z).
- [14] Masato, D., Piccolo, L., Lucchetta, G., & Sorgato, M. (2022). Texturing technologies for plastics injection molding: A review. *Micromachines*, 13(8), article number 1211. [doi: 10.3390/mi13081211](https://doi.org/10.3390/mi13081211).
- [15] McHale, G., Ledesma-Aguilar, R., & Neto, C. (2023). Cassie's law reformulated: Composite surfaces from superspreading to superhydrophobic. *Langmuir*, 39(31), 11028-11035. [doi: 10.1021/acs.langmuir.3c01313](https://doi.org/10.1021/acs.langmuir.3c01313).
- [16] Meng, Y., Xu, K., Li, S., Cao, H., Chen, C., Wei, Y., Wei, Y., & Tian, J. (2025). Slippery liquid-infused porous surfaces with long-term durable antifouling and anti-corrosion performance via bimodal structure design. *Surface and Coatings Technology*, 498, article number 131850. [doi: 10.1016/j.surfcoat.2025.131850](https://doi.org/10.1016/j.surfcoat.2025.131850).
- [17] Myronyuk, O., Baklan, D., & Rodin, A.M. (2023). UV resistance of super-hydrophobic stainless steel surfaces textured by femtosecond laser pulses. *Photonics*, 10(9), article number 1005. [doi: 10.3390/photonics10091005](https://doi.org/10.3390/photonics10091005).
- [18] Myronyuk, O., Vanagas, E., Rodin, A.M., & Wesolowski, M. (2024). Estimation of the structure of hydrophobic surfaces using the Cassie-Baxter equation. *Materials*, 17(17), article number 4322. [doi: 10.3390/ma17174322](https://doi.org/10.3390/ma17174322).
- [19] Park, I.W., Ribe, J.M., Fernandino, M., & Dorao, C.A. (2023). The criterion of the Cassie-Baxter and Wenzel wetting modes and the effect of elastic substrates on it. *Advanced Materials Interfaces*, 10(12), article number 2202439. [doi: 10.1002/admi.202202439](https://doi.org/10.1002/admi.202202439).
- [20] Peppou-Chapman, S., Hong, J.K., Waterhouse, A., & Neto, C. (2020). Life and death of liquid-infused surfaces: A review on the choice, analysis and fate of the infused liquid layer. *Chemical Society Reviews*, 49(11), 3688-3715. [doi: 10.1039/d0cs00036a](https://doi.org/10.1039/d0cs00036a).
- [21] Ramos, I., Gonçalves, M., Gonçalves, I.M., Carvalho, V., Fernandes, E., Lima, R., & Pinho, D. (2025). PDMS surface wettability modification and its applications: A systematic review. *Journal of Molecular Liquids*, 434, article number 127978. [doi: 10.1016/j.molliq.2025.127978](https://doi.org/10.1016/j.molliq.2025.127978).

- [22] Rungruangkitkrai, N., Phromphen, P., Chartvivatpornchai, N., Srissa, A., Laorenza, Y., Wongphan, P., & Harnkarnsujarit, N. (2024). Water repellent coating in textile, paper and bioplastic polymers: A comprehensive review. *Polymers*, 16(19), article number 2790. [doi: 10.3390/polym16192790](https://doi.org/10.3390/polym16192790).
- [23] Sáez-Comet, C., Fontdecaba, E., Cuadrado, N., & Puiggali, J. (2022). Injection molding and characterization of microtextures on polycarbonate using laser textured inserts. *Materials and Manufacturing Processes*, 38(5), 618-628. [doi: 10.1080/10426914.2022.2075888](https://doi.org/10.1080/10426914.2022.2075888).
- [24] Tripathi, D., Ray, P., Singh, A.V., Kishore, V., & Singh, S.L. (2023). Durability of slippery liquid-infused surfaces: Challenges and advances. *Coatings*, 13(6), article number 1095. [doi: 10.3390/coatings13061095](https://doi.org/10.3390/coatings13061095).
- [25] Xie, H., & Huang, H. (2020). Gradient wetting transition from the Wenzel to robust Cassie-Baxter states along nanopillared cicada wing and underlying mechanism. *Journal of Bionic Engineering*, 17, 1009-1018. [doi: 10.1007/s42235-020-0080-x](https://doi.org/10.1007/s42235-020-0080-x).

Формування мікротекстур полімерних поверхонь методом переносу з металевих шаблонів

Олексій Миронюк

Доктор технічних наук, доцент

Національний технічний університет України «Київський політехнічний інститут імені Ігоря Сікорського»

03056, просп. Берестейський, 37, м. Київ, Україна

<https://orcid.org/0000-0003-0499-9491>

Денис Баклан

Доктор філософії

Національний технічний університет України «Київський політехнічний інститут імені Ігоря Сікорського»

03056, просп. Берестейський, 37, м. Київ, Україна

<https://orcid.org/0000-0002-6608-0117>

Анна Білоусова

Аспірант

Національний технічний університет України «Київський політехнічний інститут імені Ігоря Сікорського»

03056, просп. Берестейський, 37, м. Київ, Україна

<https://orcid.org/0000-0002-2818-8450>

Володимир Страшенко

Аспірант

Національний технічний університет України «Київський політехнічний інститут імені Ігоря Сікорського»

03056, просп. Берестейський, 37, м. Київ, Україна

<https://orcid.org/0009-0009-3601-1821>

Анотація. Масштабування технологій створення рельєфних поверхонь з контролюваними властивостями змочування є актуальним завданням для розвитку функціональних полімерних матеріалів. Існує необхідність вивчення закономірностей перенесення мікро- та нанотекстур з металевих шаблонів на полімерні підкладки. Метою роботи було визначення впливу методу реплікації та властивостей полімеру на точність відтворення рельєфу та формування водовідштовхувальних характеристик поверхні. Для цього було використано три методи реплікації: отримання полікарбонатної плівки з розчину, реакційне формування з використанням еластомеру полідиметилсилоксану та термоформування поліетиленових плівок. Отримані негативні копії використовувалися як проміжні форми (полікарбонат) для створення позитивних реплік з поліетилену та полісилоксану. Гідрофобність матеріалів оцінювали шляхом вимірювання кутів контакту в напрямках, паралельних і перпендикулярних до орієнтації текстури. Результати показали, що всі методи забезпечують відтворення періодичних структур. Однак рівень точності залежить від в'язкості середовища та температурних умов, причому найнижчий рівень точності спостерігається для полікарбонату, а найвищий – для поліетилену. Полікарбонатні негативи характеризувалися високою деталізацією мікродефектів (до 5 мкм), тоді як поліетиленові плівки демонстрували згладжування рельєфу. Силіконові позитиви найбільш повно зберігають геометрію оригінальних текстур з дефектами. Дослідження гідрофобності поверхні показало значне збільшення кутів контакту на структурованих поверхнях порівняно з гладкими, особливо при паралельній орієнтації. Максимальні кути контакту досягали 140 °C для полісилоксану і 139 °C для поліетиленових реплік структури з регулярними канавками. Практична цінність роботи полягала у визначенні оптимальних матеріалів і методів для створення полімерних поверхонь з підвищеною водовідштовхувальною здатністю. Полікарбонат підходить для використання як проміжний матеріал для точного копіювання текстури, тоді як силікон і поліетилен мають потенціал для використання як функціональні поверхні в захисних покриттях і пористих поверхнях, просочених рідиною

Ключові слова: кут змочування; полікарбонат; силікон; поліетилен; гідрофобність